

The wall effect on the orientation of fibres in a shear flow

Allan Carlsson¹, Fredrik Lundell¹ and Daniel Söderberg²¹Department of Mechanics, School of Engineering Sciences
Royal Institute of Technology, Stockholm, Sweden² STFI - Packforsk AB, Stockholm, Sweden

ABSTRACT

An experimental study concerning the orientation of fibres in a shear flow has been performed. The shear flow is generated, by letting gravity drive a fibre suspension down an inclined plate. It is shown possible to influence the fibre orientation by modifying the surface structure of the inclined plate.

INTRODUCTION

The main intention of this study is to experimentally investigate the orientation of fibres, in a fibre suspension flowing close to a solid boundary. The fibre orientation has been determined in a plane parallel to the solid surface upon which the suspension flows. Apart from performing experiments on a plain smooth surface, experiments has also been performed on a modified structured surface, in order to see if this is a possible way of affecting the fibre orientation.

The motion of an ellipsoid suspended in a laminar simple shear flow has been solved theoretically¹. The expressions determining the motion are

$$\dot{\phi} = -\frac{\dot{\gamma}}{r_e^2 + 1}(r_e^2 \sin^2 \phi + \cos^2 \phi) \quad (1)$$

$$\dot{\theta} = \left(\frac{r_e^2 - 1}{r_e^2 + 1}\right) \frac{\dot{\phi}}{4} \sin 2\phi \sin 2\theta, \quad (2)$$

and are usually referred to as Jefferys equations. The angles θ and ϕ are defined in

Fig. 1. The shear rate is denoted by $\dot{\gamma}$ and r_e is the aspect ratio of the ellipsoid, *i.e.* the length to diameter ratio. The motion is periodic and determined by the initial conditions. The period of the motion is

$$T = \frac{2\pi}{\dot{\gamma}} \left(\frac{r_e^2 + 1}{r_e} \right). \quad (3)$$

It has been shown possible to extend Jeffery's equations to be valid for any body with a fore-aft symmetry², provided that an equivalent aspect ratio is found. In other words a relation must be found between the aspect ratio of the particle r_p and r_e . It is thus possible to use the expressions also for fibres. Experiments have been performed and have shown a good agreement with Jeffery's equations^{3, 4, 5}. However, no fibre-fibre interactions have been taken into account in Jeffery's analysis and there are no solid boundaries present.

Experiments on a simple shear flow with a solid surface present have been performed⁵. In these studies the fibre orientation was measured in a plane perpendicular to the solid surface. In a region closer than one fibre length from the surface, it was concluded that Jeffery's equations could still be applied, provided that an effective increased shear rate was used.

To the authors knowledge there is still a lack of experimental data dealing with the orientation of fibres in the plane parallel to a solid surface.

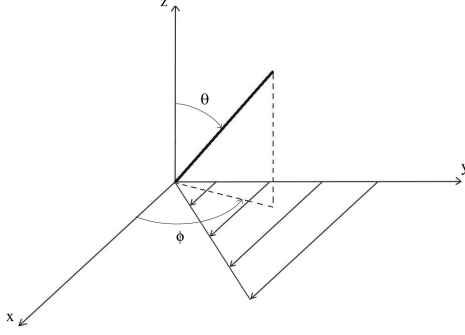


Figure 1. Coordinate system.

EXPERIMENTAL SETUP & PROCEDURE

To create a well-defined shear layer, a fibre suspension was set to flow down an inclined plate. To be able to visualize the flow the plate is constructed of glass and a CCD-camera is used to capture images of the flow. Depending on the objective, whether to find the velocity profile or to find the orientation of the fibres, the camera was mounted at different positions.

Fibre suspension

The liquid phase of the fibre suspension, used in the experiments, was a mixture of polyethyleneglycole (PEG-400) and glycerine. The temperature during the experiments was 295 ± 0.5 K. The kinematic viscosity was measured to $\nu = (383 \pm 10) \cdot 10^{-6}$ m²/s and the density to $\rho_f = 1210 \pm 15$ kg/m³.

Cellulose acetate fibres of length $l = 0.5$ mm and diameter $d = 50$ μ m was suspended into the viscous liquid. The fibres had a density of $\rho_p \approx 1300$ kg/m³. The density variation between the liquid phase and the fibres results in a sedimentation speed of the fibres with an order of magnitude of 10^{-6} m/s. The fibre concentration expressed as the number of fibres within a volume of l^3 was $nl^3 = 0.48$.

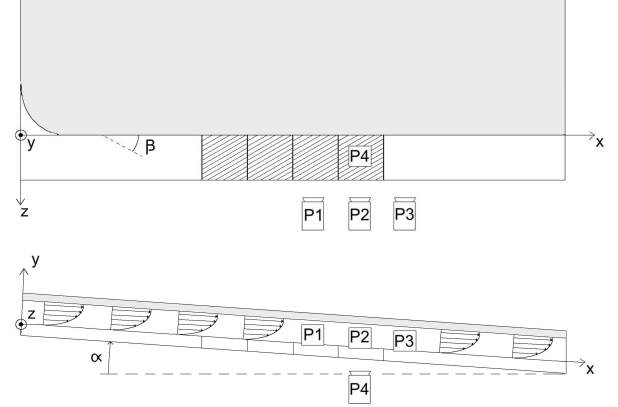


Figure 2. Schematic figure illustrating the experimental setup. P1 - P4 show the camera positions used for different objectives.

Experimental setup

The fibre suspension was allowed to flow down an inclined glass plate to generate a shear layer. A sketch of the experimental setup is shown in Fig. 2. The suspension flows in the x -direction in a 1200 mm long channel. From $x = 0$ mm to $x = 150$ mm the width of the channel changes from 400 mm to 100 mm. In the remainder of the channel the width is kept constant at 100 mm. In the initial contracted part the fibres align themselves with the flow, due to the acceleration in the flow.

Experiments were performed on two different surface structures. One plain smooth surface obtained by placing a (1200 x 100) mm² acrylic plate of height 6 mm in the channel, on top of the glass plate and another structured surface with ridges. The region in the channel from $x = 400$ mm to $x = 800$ mm was easily replaced by four (100 x 100) mm² acrylic plates of height 6 mm. On the surface facing the flow, the plates contained ridges. The ridges were oriented 30 degrees counter-clockwise to the flow direction. The shape

of the ridges was square formed with a height and width of 0.5 mm.

To visualize the flow, for orientation studies, a CCD-camera (SONY DFW-X700, 1024 x 768 pixels) was mounted underneath of the flow at $x = 750$ mm (camera position P4 in Fig. 2). A stroboscope (Drelloscop 200) was synchronized to the CCD-camera to illuminate the fibres.

Flow situation

For a viscous Newtonian fluid flowing down an inclined plate, the theoretical expression determining the velocity of the fluid is given by⁶

$$u = \frac{g}{2\nu}y(2h - y) \sin \alpha, \quad (4)$$

where g is the acceleration due to gravity, ν is the kinematic viscosity, h is the thickness of the fluid film, y is the distance from the solid surface and α is the inclination of the inclined plate with respect to the horizontal.

In the experiments the tilt angle $\alpha = 2.60 \pm 0.1$ degrees. The film thickness was measured to $h = 17.0 \pm 0.2$ mm in the region between $x = 650$ mm and $x = 850$ mm. It can thus be established that there was no global acceleration of the fluid in this region.

In order to determine the velocity profile of the fibres, the CCD-camera was mounted at the side of the flow at $x = 650$, 750 and 850 mm (camera positions P1, P2 and P3 in Fig. 2). Image analysis combined with a particle-tracking algorithm was used to determine the velocity of individual fibres, by using a series of subsequent images. In the experiments performed to determine the velocity profile, fibres of length $l = 2$ mm and diameter $d = 50 \mu\text{m}$ was used. The concentration of fibres was $nl^3 = 0.31$. The liquid containing the fibres was essentially the same as the liquid used for the orientation stud-

ies. The experiments were only performed with a smooth surface.

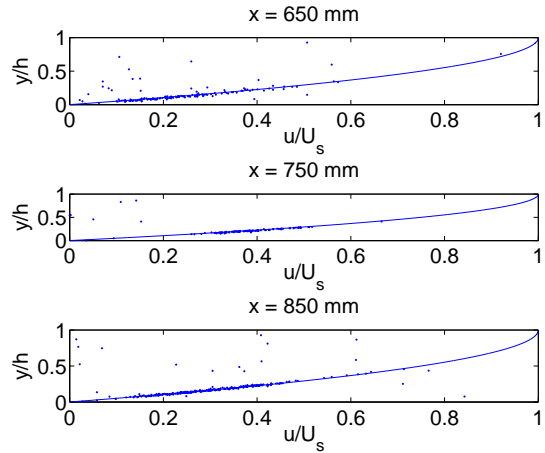


Figure 3. Velocity profiles measured at $x = 650$ mm, $x = 750$ mm and $x = 850$ mm. The dots represent experimental data and the solid line the theoretical expression, Eqn. 4.

In Fig. 3 the measured velocity profiles are presented. The dots in the figure represent individual fibres and the solid line is the theoretical expression defined in Eqn. 4. The velocity has been normalized with the theoretical velocity at the surface of the liquid film U_s and the distance from the wall is normalized with the film thickness h . Most of the dots coincide very well with the theoretical profile. However there are also dots deviating substantially from the solid line. It is believed that these dots are mismatches in the particle-tracking algorithm. If the deviating dots are disregarded it can be concluded that the velocity of the fibres strongly correlates with the distance from the solid surface.

Image Analysis

To find the orientation and position of all the fibres in a captured image, the concept of steerable filters is used⁷. The particular filter used is a 2nd order ridge detector⁸. Steerable filters is a powerful

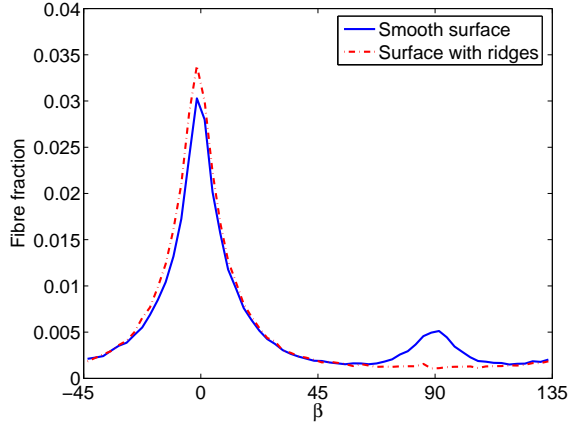


Figure 4. Fraction of fibres oriented at different angles before particle-tracking analysis has been performed.

tool, which allows the orientation of fibres to be detected in a computationally efficient way. Once the orientation and position of the fibres are found, the velocity of individual fibres can be computed in a particle-tracking algorithm. The fibres are tracked in three subsequent images, captured with a frequency $f = 10.27 \pm 0.05$ Hz.

In between every set of three images a delay of $T_s = 12$ s is implemented, allowing the majority of the fibres to leave the field of view. For fibres moving to slow, in order to pass the field of view in T_s , the area were the fibres have to be detected in the images is reduced in the flow direction. The size of the area is set so that no fibre will be detected more than once.

The total number of captured images per measuring series was 900, *i.e.* the velocity of the fibres is computed at 300 different times.

RESULTS & DISCUSSION

In Fig. 4 the probability density function of the measured fibre orientation values is presented, both for the experiments performed on the smooth surface and the surface with ridges. The angle β is de-

finied as the angle from the flow direction in the xz -plane, see Fig. 2. Fig. 4 shows the fibre fraction, before the velocity of the fibres has been computed. It is thus not possible to see how far from the solid surface the fibres are located and one fibre may be represented more than once. The number of fibres detected before the particle-tracking algorithm has been applied is 99760 for the smooth surface and 100483 for the case with ridges.

Although no information can be extracted about how far from the surface the fibres are located, it can be seen that most fibres stay aligned with flow near $\beta = 0$. Apart from the peak around $\beta = 0$, present at both surfaces, there is also a peak around $\beta = 90$ present only for the smooth surface.

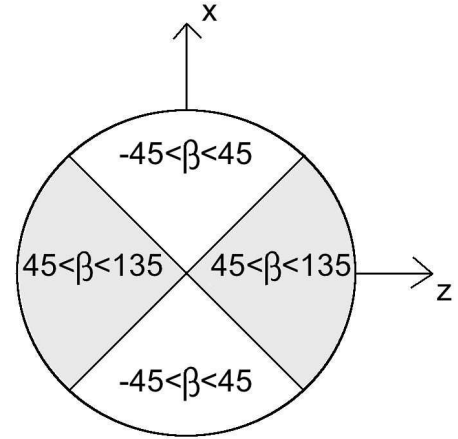


Figure 5. Orientation of fibres divided into two regions. One region around the flow direction $-45 < \beta < 45$ and one region closer to perpendicular to the flow direction $45 < \beta < 135$.

Since there are only two peaks seen in Fig. 4, the orientation of fibres is divided into two different regions for further analysis. The regions are illustrated in Fig. 5 where one region is defined as $-45 < \beta < 45$ and the other is the region

$45 < \beta < 135$. That is one region around the flow direction $\beta = 0$ and one region around the direction perpendicular to the flow $\beta = 90$.

The strong correlation between the velocity and the distance from the solid surface of the fibres, makes it possible to convert the velocity computed in the particle-tracking algorithm to a distance from the surface. It is thus possible to determine the orientation of fibres at different distances from the surface. In Fig. 6 the fraction of fibres oriented within the region $-45 < \beta < 45$, *i.e.* close to the flow direction, is shown. The distance from the surface y has been normalized with one fibre length l .

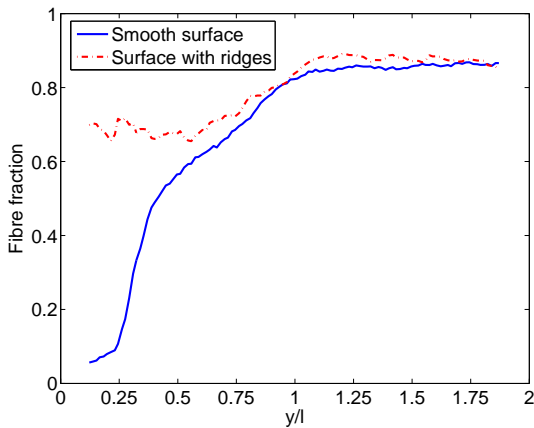


Figure 6. Fraction of fibres located in region $-45 < \beta < 45$, for different distances from the solid surface.

Closer to the wall than $l/4$ basically no fibres seem to align themselves with the flow, for the smooth surface. More than 90% of the fibres are oriented in the region $45 < \beta < 135$. As the distance from the wall increases the amount of fibres oriented close to the flow direction increases up to about one fibre length from the wall. Further away from the wall than $y = l$ the fraction of fibres oriented at $-45 < \beta < 45$ seems to be close to constant and about

80%.

As for the structured surface with ridges the fraction of fibres located in the region close to the flow direction, is also here about 80% for distances from the wall larger than one fibre length. However, closer to the surface than about $l/2$, the dashed line, corresponding to the surface with ridges, deviates from the solid line corresponding to the smooth surface. The fraction of fibres located in the region $-45 < \beta < 45$ is always more than 60% for the case with ridges.

No analysis has been carried out to determine whether there are fibres performing Jeffery orbits. Nevertheless, through observations it has been seen that there are fibres that spend most of their time aligned with the flow to occasionally flip 180 degrees around the z -axis. This is one possible solution to Eq. 1 and Eq. 2, when $\theta = \pi/2$. However the period of the motion was not measured and compared with Eq. 3.

The smallest distance to the wall where a fibre, oriented in the flow direction, could rotate around the z -axis without interfering with the solid surface is $l/2$. It is possible that this is the reason to why the lines in Fig. 6 deviates for $y < l/2$.

Another issue that has not been mentioned is how the concentration varies with the distance from the wall. In Fig. 7 the amount of detected fibres at each distance from the surface is presented. The concentration is expressed as the number of fibres present within a volume l^3 and the distance from the surface y is normalized with l .

A large peak in detected fibres is found close to the wall for the smooth surface. In the same region basically no fibres are found for case with the ridges. Although there seems to be more fibres located just outside $y = l$ for the case with ridges, the amount is too small to balance all the fi-

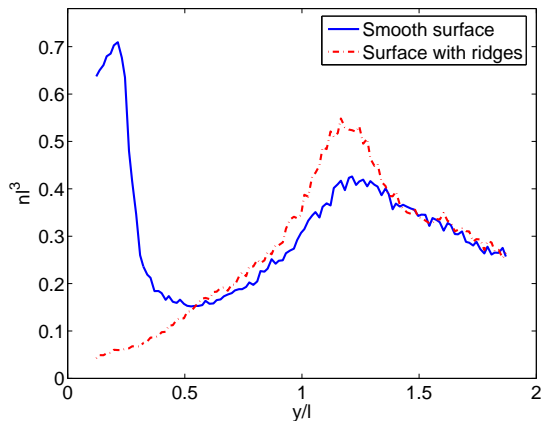


Figure 7. Variation in detected fibres for different distances from the solid surface.

bres found for $y < l/4$ for the smooth surface. The decrease in concentration, found as the distance from the surface increases, is believed to be due mainly to that the image analysis fails to detect many of the fibres in this region. The focal point of the camera is located at $y = 0$. The further away from the focal point a fibre is located the blurrier it will appear in the captured image. A blurry fibre is harder to detect in the image analysis.

It is possible to show that the size of the peak in concentration, found for the smooth surface, is about the size one could expect if sedimentation is taken into account. It is however unexpected that there are basically no fibres detected close to the surface with ridges. The most probable reason for this is that the particle-tracking algorithm fails to detect the fibres in this region.

The total number of fibres detected in the region $0 < y < 2l$, after the particle-tracking algorithm is 6932 for the smooth surface and 5375 for the surface with ridges. Before the particle-tracking algorithm the amount of detected fibres was essentially the same, for both surfaces. Thus, the reason for not finding the peak

is not that the ridges distort the captured images to reduce the number of detected fibres. It has been observed that some fibres get caught in the ridges and follow them for some time to escape again later on. Since, the particle-tracking algorithm only searches for fibres in the flow direction, it fails to detect these fibres.

Although there are a substantial amount of fibres that are not detected close to the surface with ridges, it can be concluded that the fibres in this region do not, to a large content, orient themselves perpendicular to the flow. If they were, this would give rise to a peak in Fig. 4 around $\beta = 90$.

CONCLUSIONS

The fibre orientation in a shear flow, close to a solid surface, has been studied experimentally. A fibre suspension of concentration $nl^3 = 0.48$ flowed down an inclined plate to form a shear layer. The surface of the inclined plate was changed from a plain smooth surface to a surface containing ridges, oriented 30 degrees counter-clockwise to the flow direction.

The flow was visualized with a CCD-camera located underneath the flow, for fibre orientation studies in the plane parallel to the solid surface. To measure the velocity profiles of the fibres the camera was also mounted at the side of the flow. By doing this it could be concluded that there was no acceleration in the flow and that there was a strong correlation between the velocity and the distance from the solid surface of the fibres.

For distances larger than one fibre length from the solid surface, more than 80% of the fibres were oriented in the region $-45 < \beta < 45$, where $\beta = 0$ when a fibre is oriented in the flow direction. This was seen for both different surfaces, upon which the experiments were performed on.

As the distance from the wall decreased

more fibres oriented themselves in the region $45 < \beta < 135$, for the smooth surface. For distances from the wall closer than a quarter of a fibre length more than 90% was oriented in this region.

The particle-tracking algorithm, used to determine the velocity of individual fibres, fails to detect many of the fibres close to the surface with ridges. Although it is not perfectly clear how the fibres behave, it has been possible to conclude there were not many fibres located in the region $45 < \beta < 135$, as was the case for the smooth surface.

ACKNOWLEDGEMENT

Dr. Richard Holm performed initial experiments and provided valuable input in the beginning of the project.

REFERENCES

1. G. B. Jeffery.

The motion of ellipsoidal particles immersed in a viscous fluid.

Proc. Roy. Soc. London A, pages 161–179, 1922.

2. F. P. Bretherton.

The motion of rigid particles in a shear flow at low Reynolds number.

J. Fluid Mech., 14:284–304, 1962.

3. G. I. Taylor.

The motion of ellipsoidal particles in a viscous fluid.

Proc. Roy. Soc. London A, 103:58–61, 1923.

4. R. C. Binder.

The motion of cylindrical particles in viscous flow.

J. Appl. Phys., 10:711–713, 1939.

5. K. B. Moses, S. G. Advani, and A. Reinhardt.

Investigation of fiber motion near solid boundaries in simple shear flow.

Rheol. Acta, 40:296–306, 2001.

6. D. J. Acheson.

Elementary Fluid Dynamics.

Oxford University Press, 1990.

7. W. T. Freeman and E. H. Adelson.

The design and use of steerable filters.

IEEE T. Pattern Anal., 13(9):891–906, 1991.

8. M. Jacob and M. Unser.

Design of steerable filters for feature detection using canny-like criteria.

IEEE T. Pattern Anal., 26(8):1007–1019, 2004.